Analysis of the Role of Tortuosity and Infiltration Constants in the Beerkan Method

Paolo Nasta*
Dep. of Land, Air and Water Resources
Univ. of California
Davis, CA 95618

Laurent Lassabatere
Université de Lyon
Laboratoire d'Ecologie des Hydrosystèmes Naturels et Anthropisés
UMR5023 CNRS-ENTPE-Université Lyon 1
3, rue Maurice Audin
69518 Vaulx-en-Velin, France

Maziar M. Kandelous
Dep. of Land, Air and Water Resources
Univ. of California
Davis, CA 95618

Jirka Šimůnek
Dep. of Environmental Sciences
Univ. of California
Riverside, CA 92521

Rafael Angulo-Jaramillo
Université de Lyon
Laboratoire d'Ecologie des Hydrosystèmes Naturels et Anthropisés
UMR 5023 CNRS-ENTPE-Université Lyon 1
3, rue Maurice Audin
69518 Vaulx-en-Velin, France

It has recently been proposed to couple the Beerkan method with the Beerkan Estimation of Soil Transfer parameters (BEST) algorithm to facilitate the estimation of soil hydraulic parameters from an infiltration experiment. Although this simplified field procedure is relatively rapid and inexpensive, it has been doubted if the Beerkan method can represent a valid and reliable alternative to other conventional methods. This study explored the impact of the tortuosity parameter (*p*) and two infiltration constants (β and γ) included in the BEST algorithm using a sensitivity analysis applied to three experimental soils. The analysis that was validated using the numerical model HYDRUS 2D/3D indicates that the tortuosity is relatively insignificant compared to parameters β and γ that have a large impact on the estimation procedure.

Abbreviations: BC, Brooks and Corey; HCF, hydraulic conductivity function; PSD, particle size distribution; PTF, pedotransfer function; VG, van Genuchten; WRF, water retention function.

Modeling soil hydrologic processes at hillslope or catchment scales requires knowledge of the soil hydraulic parameters for land surface layers that manifest a significant spatial variability (Ritter et al., 2003). Assessing these parameters from laboratory experiments on soil cores is often costly and time consuming (Oliver and Smettem, 2005). Moreover, because of the usually small size of soil cores, laboratory experiments can also have the drawback of identifying properties not fully representative of the effective soil hydraulic properties that control hydrologic processes at much larger spatial scales (Minasny and McBratney, 2002). For these reasons, the use of field methods seems more attractive in determining the appropriate soil hydraulic parameters (Reynolds et al., 2002; Angulo-Jaramillo et al., 2000). In general, field methods are analyzed using either analytical or numerical solutions. In the former case, however, in which only the steady-state flow rates are used, the time when steady-state conditions are reached is uncertain and this may lead to unreliable estimates of the soil hydraulic properties. In the latter case, the numerical inverse solution requires additional information, such as supplementary measurements of pressure heads or soil water contents, to ensure the parameter uniqueness (e.g., Hopmans et al., 2002).

To overcome these problems, the Beerkan method (Braud et al., 2005) was introduced to offer an alternative for estimating soil hydraulic properties while relying on different information obtainable by simple, fast, and cheap measurements (Lassabatere et al., 2006; Mubarak et al., 2009a, 2009b; Lassabatere et al., 2010; Yilmaz et al., 2010; Xu et al., 2012). This technique is based on an infiltration experiment and additional measurements of the dry bulk density, initial and saturated volumetric water contents, and the particle size distribution (PSD). The soil hydraulic properties are then estimated using the BEST algorithm (described below). Infiltration

Soil Sci. Soc. Am. J. 76:1999–2005
doi:10.2136/sssaj2012.0117n
Received 2 Apr. 2012.
*Corresponding author (paolo.nasta@unina.it).

into the soil surface horizon is assumed not to be considerably affected by preferential flow and underlying layers of the soil profile.

The BEST algorithm is based on a series of analytical expressions to calculate the soil hydraulic parameters from the aforementioned measurements. First, the shape parameters of the water retention function are estimated using a pedotransfer function (PTF) from the PSD and the dry bulk density, whereas the shape parameter of the hydraulic conductivity function depends on an unknown tortuosity parameter, p. Second, the remaining scale parameters of the water retention and hydraulic conductivity functions are determined from the analysis of measured infiltration data. Infiltration data are used in the analytical expression that describes the three-dimensional cumulative infiltration proposed by Haverkamp et al. (1994); however, the two infiltration constants (β and γ) in the analytical model are not known a priori. The objective of this study was to analyze the impact of p, β, and γ on the results obtained by the Beerkan method for three experimental soils previously investigated by Lassabatere et al. (2006). Moreover, the reliability and accuracy of the BEST algorithm, which is based on the combination of a PTF and a series of analytical solutions, may be questioned. Hence, the BEST-derived parameters were numerically validated using the HYDRUS 2D/3D model (Šimůnek et al., 2008).

THEORY

The BEST Algorithm

In the BEST algorithm, the soil water retention function, $\theta(h)$, referred to as the van Genuchten water retention function (VG-WRF), is described by van Genuchten's equation (van Genuchten, 1980):

$$\theta(h)=\theta_r+\frac{\theta_s-\theta_r}{\left[1+(\alpha|h|)^n\right]^m} \qquad [1a]$$

with Burdine's condition (Burdine, 1953):

$$m=1-\frac{2}{n} \qquad [1b]$$

where α [L^{-1}] is a scale parameter for the pressure head, h [L], which is equal to the reciprocal of the inflection point (h_g) of the water retention curve ($h_g = 1/\alpha$), θ_r [$L^3\ L^{-3}$] and θ_s [$L^3\ L^{-3}$] are the residual and saturated water contents, respectively, and n and m are dimensionless retention curve shape parameters. The unsaturated hydraulic conductivity function, $K(\theta)$, referred to as the Brooks and Corey hydraulic conductivity function (BC-HCF), is described by the relationship proposed by Brooks and Corey (1964):

$$K(\theta)=K_s\left(\frac{\theta-\theta_r}{\theta_s-\theta_r}\right)^\eta \qquad [2]$$

where K_s [$L\ T^{-1}$] is the saturated hydraulic conductivity and η is a dimensionless conductivity shape parameter that is related to the retention curve shape parameters through the following equation, expressing the capillary model:

$$\eta=\frac{2}{mn}+2+p \qquad [3]$$

where p (dimensionless) is a tortuosity parameter that is assumed to be equal to 0 (Childs and Collis-George, 1950), 0.5 (Mualem, 1976), 1.0 (Burdine, 1953), or 1.33 (Millington and Quirk, 1961). In the original procedure of Lassabatere et al. (2006), p was set according to Burdine's condition ($p = 1.0$). In the BEST algorithm, it is also assumed that the residual water content (θ_r) is equal to zero (Haverkamp et al., 2005; Leij et al., 2005).

The Beerkan method requires that an undisturbed soil core is collected to measure the dry bulk density, ρ_b [$M\ L^{-3}$], the initial volumetric water content, θ_0 [$L^3\ L^{-3}$], the saturated volumetric water content, θ_s [$L^3\ L^{-3}$], and the PSD. Subsequently, the experimental cumulative infiltration is measured using an annular ring of radius r_d [L], with a constant zero pressure head at the soil surface. A series of known volumes of water is poured into the cylinder and the time is recorded when the water has infiltrated into the soil. The BEST algorithm uses the experimental cumulative infiltration, I_{EXP} [L], expressed per unit area of the annular ring for each time, t_k [T].

The BEST algorithm starts with a PTF, which is used to estimate the shape parameters (n, m, and η) from the PSD and ρ_b measurements (Braud et al., 2005; Lassabatere et al., 2006). Subsequently, the analytical solution for three-dimensional infiltration (I_{BEST}), valid for the transient state, is used (Haverkamp et al., 1994):

$$I_{BEST}(t)=S\sqrt{t}+\left[A(1-B)S^2+Bq_{+\infty}\right]t \qquad [4]$$

with

$$\begin{cases} A=\dfrac{\gamma}{r_d(\theta_s-\theta_0)} \\ B=\dfrac{2-\beta}{3}\left[1-\left(\dfrac{\theta_0}{\theta_s}\right)^\eta\right]+\left(\dfrac{\theta_0}{\theta_s}\right)^\eta \end{cases} \qquad [5]$$

where S [$L\ T^{-1/2}$] is the sorptivity, $q_{+\infty}$ [$L\ T^{-1}$] is the steady-state infiltration rate, assumed to be the asymptotic slope of the last few experimental data points, β (dimensionless) adjusts the relation between the water diffusivity and the unsaturated hydraulic conductivity, and γ (dimensionless) corrects the analytical three-dimensional infiltration equation (Eq. [4]) for the effects of radial expansion (Fuentes et al., 1992; Haverkamp et al., 1994). The constant γ is feasible in the range of $0.6 < \gamma < 0.8$ (Haverkamp et al., 1994), while β was originally constrained in the interval of $0 < \beta < 1$ (Fuentes et al., 1992; Haverkamp et al., 1994; Braud et al., 2005). Subsequently, Lassabatere et al. (2009) considered a larger range of β ($0 < \beta < 2$) to evaluate its effect on the accuracy of the three-dimensional analytical solution with respect to numerically generated three-dimensional cumulative

infiltration for four synthetic soils. Lassabatere et al. (2006) used the BEST algorithm, assuming that $\gamma = 0.75$ and $\beta = 0.60$ for three experimental soils. It is still necessary, however, to better understand the effect of these infiltration constants, along with the tortuosity parameter, p, on the estimates of the soil hydraulic parameters.

The sorptivity (S_k) is obtained by incrementally minimizing the sum of squared deviations between the experimental data (cumulative infiltration, $I_{EXP,k}$, at time t_k) and the analytical solution given by Eq. [4] (cumulative infiltration, $I_{BEST,k}$, at time t_k) (Lassabatere et al., 2006). The selection of the final value of the sorptivity (S) from the series of S_k values depends on the maximum transient time, $t_{max}(k)$ [T], which corresponds to the upper limit of the validity interval of Eq. [4] (Lassabatere et al., 2006):

$$t_{max}(k)=\frac{1}{4(1-B)^2}\left(\frac{S_k}{q_{+\infty}-AS_k^2}\right)^2 \qquad [6]$$

The final value of S is chosen for the largest experimental time, t_k, that fulfills the condition $t_{max}(k) \geq t_k$. This condition offers an empirical, but relatively robust, selection of data during the transient phase of the cumulative infiltration curve. The saturated hydraulic conductivity, K_s, is then given by the analytical solution for the steady-state condition:

$$K_s = q_{+\infty} - AS^2 \qquad [7]$$

Finally, the retention curve scale parameter, h_g [L], is calculated using

$$h_g = -\frac{S^2}{c_p K_s (\theta_s - \theta_0)\left[1-(\theta_0/\theta_s)^{\eta}\right]} \qquad [8]$$

where c_p (dimensionless) is a texture-dependent parameter retrieved from the shape parameters of the soil hydraulic functions (Braud et al., 2005; Lassabatere et al., 2006).

Numerical Model

The infiltration experiments were consequently modeled using HYDRUS 2D/3D, which numerically solves the Richards equation describing water flow in a variably saturated, isotropic, rigid, porous medium (Šimůnek et al., 2008):

$$\frac{\partial\theta}{\partial t}=\frac{1}{r}\frac{\partial}{\partial r}\left(rK\frac{\partial h}{\partial r}\right)+\frac{\partial}{\partial z}\left[K(h)\frac{\partial h}{\partial z}\right]+\frac{\partial K}{\partial z} \qquad [9]$$

where r is the radial coordinate [L] and z is the vertical coordinate [L], positive upward. The surface soil layer was represented by a three-dimensional, axisymmetric, finite-element mesh with both depth and radius of 300 mm. The initial and boundary conditions were:

$$h(r,z,t)=h_0 \quad t=0,\ r>0,\ z<0 \qquad [10a]$$

$$h(r,z,t)=0 \quad t>0,\ 0<r<r_d,\ z=0 \qquad [10b]$$

$$q(r,z,t)=0 \quad t>0,\ r>r_d,\ z=0 \qquad [10c]$$

where $z = 0$ is the surface of the soil surface layer, and h_0 is the uniform initial matric head in the soil layer derived from the measured initial water content, θ_0, by inverting Eq. [1a]. Infiltration was modeled on the part of the soil surface delimited by the ring (with radius r_d) using the zero pressure head boundary condition (Eq. [10b]), while the remaining area outside of the ring had the zero water flux ($q = 0$) boundary condition (Eq. [10c]). Free drainage was set at the bottom of the modeled transport domain.

Because HYDRUS 2D/3D does not support the combination of soil hydraulic properties given by Eq. [1] (VG-WRF) and Eq. [2] (BC-HCF) as required by the BEST algorithm, its Look-up Table option was adapted to provide the definition of the soil hydraulic properties (Table 1) using an external text input file, *Mater.in*.

We emphasize that both the BEST algorithm and the HYDRUS 2D/3D model were set up assuming a homogenous soil profile with negligible effects of heterogeneity. Moreover, the unimodal parametric relationships (Eq. [1] and [2]) adopted in the analytical BEST algorithm are not able to capture the presence of macropores in the investigated porous medium (e.g., Kodešová et al., 2006; Akay et al., 2008). Bimodal forms of the soil hydraulic properties would certainly be more suitable to describe possible effects of macroporosity (e.g., Durner, 1994). Although HYDRUS 2D/3D is capable of considering the bimodal soil hydraulic model of Durner (1994), the analysis was performed using the unimodal parametric relations (Eq. [1] and [2]) to be consistent with the constraints of the BEST algorithm.

RESULTS AND DISCUSSION

The Beerkan infiltration experiments reported in Lassabatere et al. (2006) were performed on three soils: Roujan (loam), Chernobyl (sand), and Django Reinhardt (sand). Table 1 provides the

Table 1. Original properties and parameters for the three experimental soils (Lassabatere et al., 2006).

Parameter	Roujan	Chernobyl	Django Reinhardt
Sand, %	40.57	91.17	98.28
Silt, %	43.73	8.81	1.71
Clay, %	15.70	0.02	0.01
Annular ring radius (r_d), mm	75	75	100
Initial water content (θ_0), $m^3\ m^{-3}$	0.030	0.063	0.050
Saturated water content (θ_s), $m^3\ m^{-3}$	0.330	0.314	0.400
Retention curve shape parameter n	2.20	2.97	2.65
Retention curve shape parameter m	0.089	0.327	0.246
Conductivity shape parameter η	13.20	5.06	6.07
Steady-state infiltration rate ($q_{+\infty}$), mm s^{-1}	1.60×10^{-2}	2.15×10^{-2}	6.91×10^{-2}
Maximum transient time (t_{max}), s	12,770	1768	93
Sorptivity (S), mm $s^{-0.5}$	0.579	0.507	0.630
Saturated hydraulic conductivity (K_s), mm s^{-1}	4.79×10^{-3}	1.03×10^{-2}	6.33×10^{-2}
Retention curve scale parameter (h_g), mm	−99.5	−61.8	−9.6

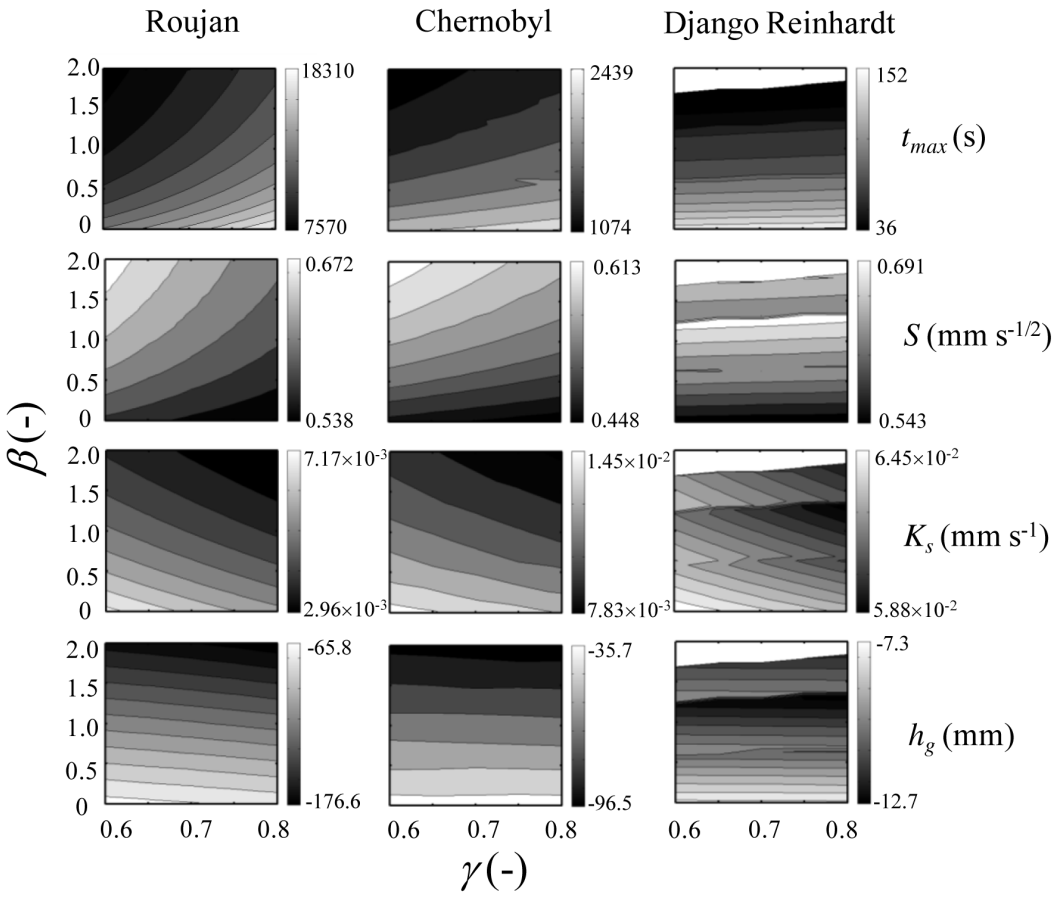

Fig. 1. The effect of infiltration constants β and γ on the estimates of the maximum transient time, t_{max}, sorptivity, S, saturated hydraulic conductivity, K_s, and retention curve scale parameter, h_g for Roujan, Chernobyl, and Django Reinhardt soils. Note that the tortuosity parameter is set to its original value (p = 1).

textural and experimental characteristics and originally estimated hydraulic parameters that describe the surface soil layer (measured PSDs were depicted in Lassabatere et al., 2006, Fig. 1).

Impact of Tortuosity and Infiltration Constants in the BEST Algorithm

After estimation of the water retention shape parameters (n and m), the tortuosity parameter (p) was used to calculate the hydraulic conductivity shape parameter (η) in Eq. [3]. Table 2 reports the basic statistical properties for the shape parameter η (mean, standard deviation, and coefficient of variation) that were derived from the four different values of p (0, 0.5, 1.0, and 1.33). Because p is additive in Eq. [3], its variability has more weight for lower η values, hence for the sandy soils. The variability of η as a function of p is rather low, however, as evidenced by the low coefficient of variation (Table 2).

For experimental conditions with initially dry soils, when $\theta_0 << \theta_s$ and thus $(\theta_0/\theta_s)^{\eta} \sim 0$, the low impact of p can be explained by the following approximation of the three-dimensional infiltration Eq. [4] and [5]:

$$I_{\mathrm{BEST}}(t) = S\sqrt{t} + \left[\frac{\gamma}{r_d(\theta_s-\theta_0)}\left(1-\frac{2-\beta}{3}\right)S^2 + \frac{2-\beta}{3}q_{+\infty}\right]t \quad [11]$$

Equation [11] does not depend on η (and on the tortuosity, p), which thus has a negligible impact on the optimization of S and consequently on the estimation of K_s (Eq. [7]) and h_g (Eq. [8]). For the scale parameter h_g, however, we emphasize that the varia-

Table 2. Mean, standard deviation (SD), and coefficient of variation (CV) of the analyzed soil hydraulic parameters for the three experimental soils.

Parameter	Roujan			Chernobyl			Django Reinhardt		
	Mean	SD	CV	Mean	SD	CV	Mean	SD	CV
			%			%			%
Conductivity shape parameter η	12.92	0.58	4.5	4.77	0.58	12.21	5.78	0.58	10.08
Maximum transient time (t_{max}), s	11,107	2248	20.2	1586	317	19.9	77.6	33.4	43.0
Sorptivity (S), mm s$^{-0.5}$	0.605	0.031	5.1	0.538	0.040	7.4	0.629	0.036	5.7
Saturated hydraulic conductivity (K_s), mm s^{-1}	4.62×10^{-3}	9.69×10^{-4}	20.9	1.08×10^{-2}	1.60×10^{-3}	14.8	6.17×10^{-2}	1.20×10^{-3}	2.0
Retention curve scale parameter (h_g), mm	−119.2	30.2	25.4	−65.9	17.3	26.3	−10.1	1.3	12.7

tion of the texture-dependent parameter c_p as a function of p in its feasible range between 0 and 1.33 is not significant in Eq. [8].

For the reasons stated above, the BEST algorithm was run for the three soils with only the original value of η (Table 1), resulting from the assumption of $p = 1$ (Burdine's condition), as in Lassabatere et al. (2006), while varying the constant β in the feasible range of $0 < \beta < 2$ and the proportionality constant γ in the feasible range of $0.6 < \gamma < 0.8$. The results of these calculations for the parameters t_{max}, S, K_s, and h_g are presented in Fig. 1. Table 2 reports the comprehensive descriptive statistics of the sensitivity analysis. The maximum transient time, t_{max} (Eq. [6]), was rather variable for all three soils and tended to increase for decreasing values of β and increasing values of γ. On the other hand, the sorptivity showed the opposite trend as a function of β and γ compared with t_{max} and is characterized by the lowest variability (see Table 2). A closer inspection of Eq. [7] reveals the role of the term A (which includes the infiltration constant γ in Eq. [5]), which affects the sorptivity under steady-state conditions and subsequently K_s.

The water retention scale parameter, h_g, is influenced mainly by the parameter β in so far as its values show a clear horizontal pattern that increases with decreasing β values. This observation confirms the theoretical statements of Fuentes et al. (1992, Fig. 1). The Django Reinhardt soil, however, compared with the other two soils, exhibited only minor variations of t_{max}, S, K_s, and h_g as a function of γ because the infiltration process in this soil is driven mainly by gravity and the radial correction of the infiltration had only very minor effects on the results. The parameter γ corrects the simplified theoretical description of the parabolic two-dimensional wetting front and the one-dimensional wetting front along the soil profile (see Smettem et al., 1994, Fig. 1). On the other hand, β influences the shape of the soil water diffusivity and, consequently, of the soil hydraulic curves (Fuentes et al., 1992). Therefore, we can attribute a geometric meaning to γ and a structural meaning to β.

Numerical Validation

The original parameters reported in Table 1 were used in HYDRUS 2D/3D to obtain the simulated cumulative infiltration curves (I_{HYDRUS}) that are compared graphically in Fig. 2a with the corresponding experimental data (I_{EXP} for N data points at times t_k) and numerically using the root mean squared errors (RMSEs):

$$\text{RMSE} = \sqrt{\frac{\sum_{k=1}^{N}\left[I_{HYDRUS}(t_k) - I_{EXP}(t_k)\right]^2}{N}} \qquad [12]$$

The RMSEs that are reported for each soil in Fig. 2a indicate good agreement between measured and simulated cumulative infiltration curves. Small deviations (reflected by low RMSE values) imply that the BEST-derived soil hydraulic parameters were able to numerically generate infiltration curves that are approximately similar to the experimental data.

Figure 2b shows the water content profiles for the three soils at the initial time (t_0), maximum transient time (t_{max}), and final experimental time (t_{end}). We note that $t_{max} > t_{end}$ for the Roujan soil, which clearly indicates that the experiment was terminated prematurely. This was also demonstrated by a significant radial expansion of the moisture front outside of the ring, which im-

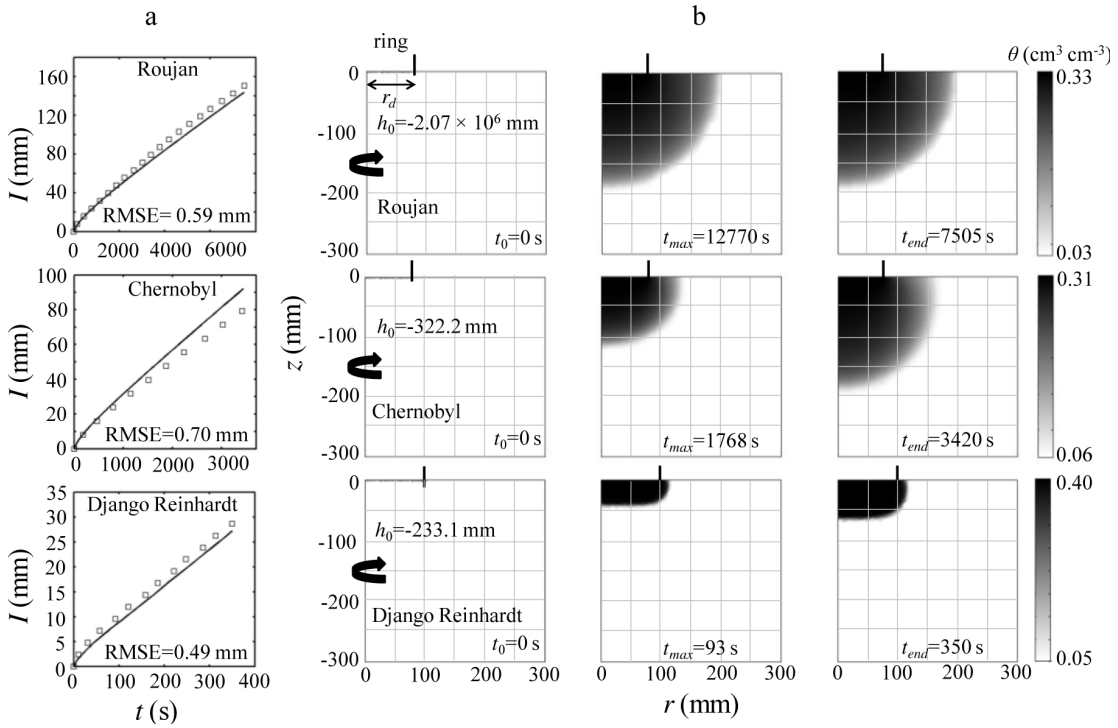

Fig. 2. (a) Infiltration curves simulated using HYDRUS 2D/3D (I_{HYDRUS}) (lines) with parameters reported in Table 1 compared with the experimental data (I_{EXP}) (symbols); (b) soil water content profiles simulated using HYDRUS 2D/3D at time 0 (t_0), maximum transient time (t_{max}), and final time of the experiment (t_{end}) for Roujan, Chernobyl, and Django Reinhardt soils.

plies that capillary forces dominated over gravity during the infiltration experiment in this particular soil. On the contrary, we can observe that water tended to mainly infiltrate in the vertical direction after a short time in the coarser soils (i.e., Django Reinhardt and Chernobyl).

Finally, we numerically evaluated with HYDRUS 2D/3D the results generated using the BEST algorithm for different combinations of the parameters p, β, and γ that determined the variability of the following soil hydraulic parameters: η, h_g, and K_s. We note that the other BEST parameters (θ_s, n, and m) were kept constant throughout the entire analysis. One numerical HYDRUS 2D/3D simulation was performed for each set of soil hydraulic parameters (η, h_g, and K_s) estimated using the BEST algorithm for the corresponding set of parameters (p, β, and γ).

The RMSEs between modeled (I_{HYDRUS}) and experimental (I_{EXP}) cumulative infiltration data were calculated using Eq. [12]. Figure 3 shows the relative deviations from the minimum RMSE, RD (%), given by

$$RD=\frac{\left[RMSE-\min(RMSE)\right]}{\min(RMSE)} \qquad [13]$$

where min(RMSE) is the minimum RMSE across all the sets of parameters (p, γ, β). The stars in Fig. 3 indicate that the originally considered values of the infiltration constants, i.e., $\gamma = 0.75$ and $\beta = 0.60$, were not optimal for the three experimental soils; however, the inaccuracy caused by p, β, and γ did not significantly affect the final estimates of the soil hydraulic parameters (η, h_g, and K_s) with regard to numerical modeling because all the RD values are <10%. The sensitivity analysis also confirmed that the impact of the tortuosity parameter p (varying in the feasible range from 0–1.33) on the final results was negligible.

In Fig. 3, the minimum RMSE values are located at different positions in the subplots for each experimental soil. We therefore believe that to further improve the final estimates by the BEST algorithm and to reduce the uncertainty in the estimated parameters, a specific calibration of β and γ for each soil type would be required. We also note that the first part of the BEST algorithm, in which the shape parameters of the VG-WRF (n and m) are estimated from the PSD and the soil bulk density using a PTF, was skipped in this study. The performance of this PTF has been already successfully verified on large experimental databases (Minasny and McBratney, 2007).

CONCLUSION

The Beerkan method is an alternative technique to conventional laboratory or field measurements for rapid and low-cost estimation of soil hydraulic properties that is based on trustworthy and robust analytical solutions. In this technical note, we have assessed the sensitivity analysis of the BEST algorithm regarding the choice of tortuosity (p) and infiltration constants (γ and β) in their feasible range. The results demonstrate that tortuosity (p) plays only a secondary role compared with constants β and γ, which are more important for the estimation of the scale parameters.

Numerical simulations performed using HYDRUS 2D/3D with the soil hydraulic parameters estimated by the Beerkan method (Lassabatere et al., 2006) provided a good description of experimental cumulative infiltration curves, indicating reliability of this technique. We offered an interpretation of the role of the two infiltration constants, highlighting the pros and cons that characterize the Beerkan method. The proper calibration of these two constants, as a function of the soil type, could significantly further improve the estimates of the soil hydraulic parameters.

We therefore conclude that, for soil surface horizons not significantly affected by macroporosity or preferential flow, the soil hydraulic parameters derived using the

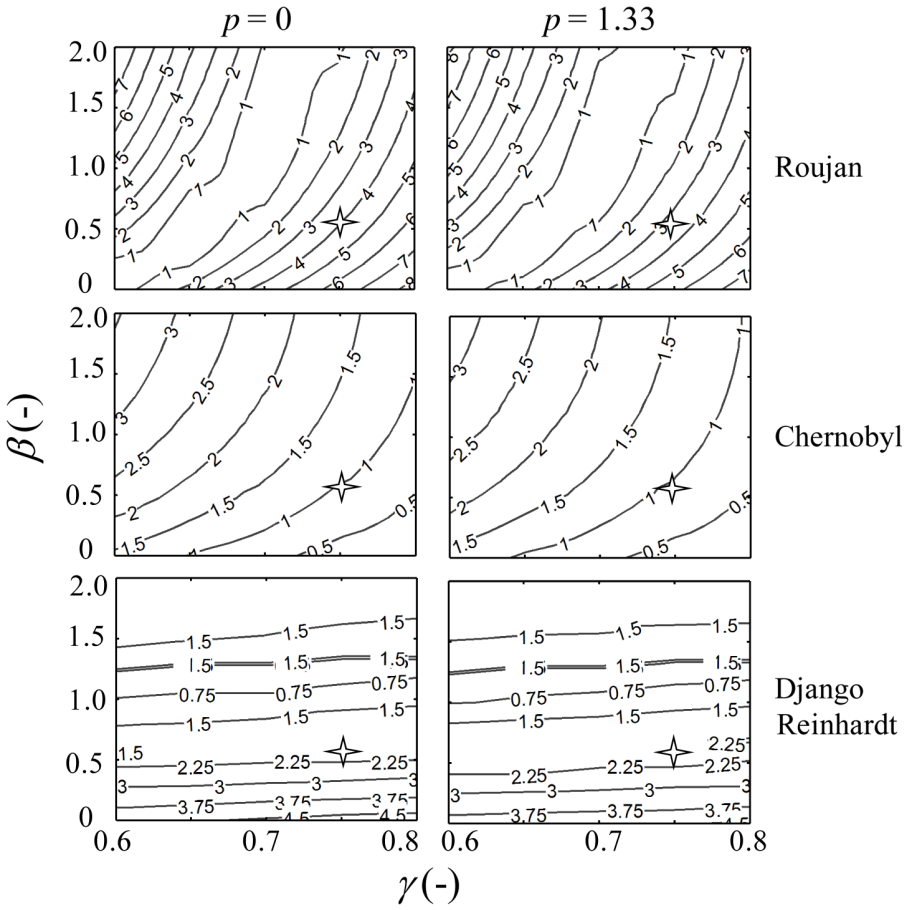

Fig. 3. Relative differences (in %, with respect to the minimum RMSE) as a function of infiltration constants β and γ and tortuosity parameter p (results are shown only for two limiting values of p and not for 0.5 and 1) for the Roujan, Chernobyl, and Django Reinhardt soils. The stars indicate the positions corresponding to $\gamma = 0.75$ and $\beta = 0.60$.

BEST algorithm can be utilized in numerical models to accurately describe water infiltration.

ACKNOWLEDGMENTS

Paolo Nasta would like to thank Dr. Massimo Nicolazzo and Dr. William Piras for their technical support.

REFERENCES

Akay, O., G.A. Fox, and J. Šimůnek. 2008. Numerical simulation of flow dynamics during macropore–subsurface drain interactions using HYDRUS. Vadose Zone J. 7:909–918. doi:10.2136/vzj2007.0148

Angulo-Jaramillo, R., J.-P. Vandervaere, S. Roulier, J.-L. Thony, J.-P. Gaudet, and M. Vauclin. 2000. Field measurement of soil surface hydraulic properties by disc and ring infiltrometers: A review and recent developments. Soil Tillage Res. 55:1–29. doi:10.1016/S0167-1987(00)00098-2

Braud, I., D. De Condappa, J.M. Soria Ugalde, R. Haverkamp, R. Angulo-Jaramillo, S. Galle, and M. Vauclin. 2005. Use of scaled forms of the infiltration equation for the estimation of unsaturated soil hydraulic properties (the Beerkan method). Eur. J. Soil Sci. 56:361–374. doi:10.1111/j.1365-2389.2004.00660.x

Brooks, R.H., and C.T. Corey. 1964. Hydraulic properties of porous media. Hydrol. Pap. 3. Colorado State Univ., Fort Collins.

Burdine, N.T. 1953. Relative permeability calculations from pore-size distribution data. Trans. Am. Inst. Min. Eng. 198:71–78.

Childs, E.C., and N. Collis-George. 1950. The permeability of porous materials. Proc. R. Soc., Ser. A 201:392–405. doi:10.1098/rspa.1950.0068

Durner, W. 1994. Hydraulic conductivity estimation for soils with heterogeneous pore structure. Water Resour. Res. 30:211–223. doi:10.1029/93WR02676

Fuentes, C., R. Haverkamp, and J.-Y. Parlange. 1992. Parameter constraints on closed-form soil water relationships. J. Hydrol. 134:117–142. doi:10.1016/0022-1694(92)90032-Q

Haverkamp, R., F.J. Leij, C. Fuentes, A. Sciortino, and P.J. Ross. 2005. Soil water retention: I. Introduction of a shape index. Soil Sci. Soc. Am. J. 69:1881–1890. doi:10.2136/sssaj2004.0225

Haverkamp, R., P.J. Ross, K.R.J. Smettem, and J.-Y. Parlange. 1994. Three-dimensional analysis of infiltration from the disc infiltrometer: 2. Physically based infiltration equation. Water Resour. Res. 30:2931–2935. doi:10.1029/94WR01788

Hopmans, J.W., J. Šimůnek, N. Romano, and W. Durner. 2002. Inverse methods. In: J.H. Dane and G.C. Topp, editors, Methods of soil analysis. Part 4. SSSA Book Ser. 5. SSSA, Madison, WI. p. 963–1008.

Kodešová, R., J. Kozák, and J. Šimůnek. 2006. Numerical study of macropore impact on ponded infiltration in clay soils. Soil Water Res. 1:16–22.

Lassabatere, L., R. Angulo-Jaramillo, D. Goutaland, L. Letellier, J.P. Gauder, T. Winiarski, and C. Delolme. 2010. Effect of the settlement of sediments on water infiltration in two urban infiltration basins. Geoderma 156:316–325. doi:10.1016/j.geoderma.2010.02.031

Lassabatere, L., R. Angulo-Jaramillo, J.M. Soria Ugalde, R. Cuenca, I. Braud, and R. Haverkamp. 2006. Beerkan estimation of soil transfer parameters through infiltration experiments—BEST. Soil Sci. Soc. Am. J. 70:521–532. doi:10.2136/sssaj2005.0026

Lassabatere, L., R. Angulo-Jaramillo, J.M. Soria-Ugalde, J. Šimůnek, and R. Haverkamp. 2009. Numerical evaluation of a set of analytical infiltration equations. Water Resour. Res. 45:W12415. doi:10.1029/2009WR007941

Leij, F.J., R. Haverkamp, C. Fuentes, Z. Zatarain, and P.J. Ross. 2005. Soil water retention: II. Derivation and application of shape index. Soil Sci. Soc. Am. J. 69:1891–1901. doi:10.2136/sssaj2004.0226

Millington, R.J., and J.P. Quirk. 1961. Permeability of porous solids. Trans. Faraday Soc. 57:1200–1206. doi:10.1039/tf9615701200

Minasny, B., and A.B. McBratney. 2002. The efficiency of various approaches to obtaining estimates of soil hydraulic properties. Geoderma 107:55–70. doi:10.1016/S0016-7061(01)00138-0

Minasny, B., and A.B. McBratney. 2007. Estimating the water retention shape parameter from sand and clay content. Soil Sci. Soc. Am. J. 71:1105–1110. doi:10.2136/sssaj2006.0298N

Mualem, Y. 1976. A new model for predicting the hydraulic conductivity of unsaturated porous media. Water Resour. Res. 12:513–522. doi:10.1029/WR012i003p00513

Mubarak, I., J. C. Mailhol, R. Angulo-Jaramillo, S. Bouarfa, and P. Ruelle. 2009a. Effect of temporal variability in soil hydraulic properties on simulated water transfer under high-frequency drip irrigation. Agric. Water Manage. 96:1547–1559.

Mubarak, I., J.C. Mailhol, R. Angulo-Jaramillo, P. Ruelle, and M. Khaledian. 2009b. Temporal variability in soil hydraulic properties under drip irrigation. Geoderma 150:158–165. doi:10.1016/j.geoderma.2009.01.022

Oliver, Y.M., and K.R.J. Smettem. 2005. Predicting water balance in a sandy soil: Model sensitivity to the variability of measured saturated and near saturated hydraulic properties. Aust. J. Soil Res. 43:87–96. doi:10.1071/SR03146

Reynolds, W.D., D.E. Elrick, E.G. Youngs, A. Amoozegar, H.W.G. Booltink, and J. Bouma. 2002 Saturated and field-saturated water flow parameters. In: J.H. Dane and G.C. Topp, editors, Methods of soil analysis. Part 4. SSSA Book Ser. 5. SSSA, Madison, WI. p. 797–878.

Ritter, A., F. Hupet, R. Munoz-Carpena, S. Lambot, and M. Vanclooster. 2003. Using inverse methods for estimating soil hydraulic properties from field data as an alternative to direct methods. Agric. Water Manage. 59:77–96. doi:10.1016/S0378-3774(02)00160-9

Šimůnek, J., M.Th. van Genuchten, and M. Šejna. 2008. Development and applications of the HYDRUS and STANMOD software packages and related codes. Vadose Zone J. 7:587–600. doi:10.2136/vzj2007.0077

Smettem, K.R.J., J.-Y. Parlange, P.J. Ross, and R. Haverkamp. 1994. Three-dimensional analysis of infiltration from the disc infiltrometer: 1. A capillary-based theory. Water Resour. Res. 30:2925–2929. doi:10.1029/94WR01787

van Genuchten, M.Th. 1980. A closed form equation for predicting the hydraulic conductivity of unsaturated soils. Soil Sci. Soc. Am. J. 144:892–898.

Xu, X., C. Lewis, W. Liu, J.D. Albertson, and G. Kiely. 2012. Analysis of single-ring infiltrometer data for soil hydraulic properties estimation: Comparison of BEST and Wu methods. Agric. Water Manage. 107:34–41. doi:10.1016/j.agwat.2012.01.004

Yilmaz, D., L. Lassabatere, R. Angulo-Jaramillo, D. Deneele, and M. Legret. 2010. Hydrodynamic characterization of basic oxygen furnace slag through an adapted BEST method. Vadose Zone J. 9:107–116. doi:10.2136/vzj2009.0039